Thermal stability of reactive sputtered silicon-doped diamond-like carbon films

Kyoung-Hoon Er[a] and Myoung-Gi So[b],*

[a]*Department of Surface Finishing, Chuncheon Campus of Korea Polytechnic III, 72 Udu-dong, Chuncheon, Gangwon-do, 200-150, Republic of Korea*
[b]*Department of Advanced Materials Science and Engineering, Kangwon National University, Chuncheon, Gangwon-do, 200-701, Republic of Korea*

Silicon doped diamond-like carbon (Si-DLC) thin films with Si contents in the 0-15 at.% range were deposited on silicon substrates using a reactive-sputtering method. The thermal stability of the films was investigated by 1 h open-air tube furnace heat treatment from 200 °C to 700 °C at intervals of 100 °C. The thickness changes and structural modification of the annealed films as a function of annealing temperature were closely studied. Raman spectroscopy and cross-sectional FESEM images were used to determine the structure and thickness changes of the annealed pure DLC and Si-DLC films, respectively. It was found that, as the Si content was increased, the graphitization (sp^3-to-sp^2 transition) temperature increased and the thickness loss decreased, which reflected the good thermal stability of the Si-DLC films. The tribological behaviors of the films, as evaluated using a ball-on-disk tribometer, reflected the property of low friction.

Key words : Si-DLC, thin films, reactive sputtering, thermal stability, microstructure.

Introduction

Silicon doped diamond-like carbon (Si-DLC) films have attracted increasing research attention for their significant potential utility in solving some of the inherent drawbacks (e.g. high internal stress, low thermal stability) of pure DLC films [1, 2]. Incorporation of Si into DLC films improves film adhesion, film strength, and further improves thermal stability by promoting sp^3-hybridized bond formation, specifically through modification of the chemical bonding configuration of a-C : H film [3]. Although Si-DLC films have been fabricated by various means, the usual synthesis methods are a combined plasma-assisted PVD/CVD technique and a sputtering system [4, 5]. Recently, application of nanocomposite DLC coatings by magnetron sputtering has been the focus of intense interest for its easy industrial-use up-scaling [6, 7] and efficacy for roughness improvement without any loss of tribological properties [8].

As for the thermal stability of metal doped DLC (Me-DLC), it is well known that it can be used to form two-dimensional arrays of nanocrystalline metal clusters and metallic carbides embedded in a carbon matrix [9]. However, to date, no systematic attempt has been made to examine the microstructure-related thermal stability and mechanical properties of magnetron-sputtering produced Si-DLC films as a function of silicon concentration. Recently, Yang et al. [10] observed a no remarkable thickness decrease of diamond-like nanocomposite (Si-O doping) films upon high temperature annealing. Varma et al. [11] investigated the structure-property relationship of Si-DLC films prepared by the ion beam-assisted deposition (IBAD) technique, finding them to be of mainly amorphous structure wherein domains with distorted sp^3 and sp^2 bonding co-exist, however, they did not observe the thermal stability of those films.

Therefore, in the present work, the thermal stability of hydrogenated sputtered Si-DLC films was studied by annealing them in ambient air. The annealing temperatures effects on the Si-DLC films' microstructure in terms of thickness changes and structural modification were investigated.

Experimental

Pure DLC and Si-DLC films were deposited on a p-type Si (100) substrate using a reactive-sputtering system, entailing plasma decomposition of a CH_4-SiH_4 (5% in Ar) gas mixture and RF magnetron sputtering of a high purity (99.99%) graphite target by Argon. The specifications on the reactive-sputtering system have been reported elsewhere [12]. The substrates were not heated or biased during the deposition, but the deposition time was varied to achieve films of about 500 nm thickness with the different deposition rates. The Si content was controlled by varying the SiH_4 flow rate from 0 (pure DLC), to 4.49 and to 9.17 sccm. The Si contents in the Si-DLC films as determined by X-

*Corresponding author:
 Tel : +82 33 250 6265
 Fax: +82 33 250 6260
 E-mail: mgso@kangwon.ac.kr

ray photoelectron spectroscopy (XPS) were 7 at.% and 15 at.%, respectively [12]. Subsequently, all of sputtered films were 1h open-air tube furnace heat-treated from 200 °C to 700 °C at intervals of 100 °C in order to study their thermal stability. After unloading from the furnace, the films were cooled to room temperature in ambient air. Cross-sectional FESEM images were then employed in the measurement of the film thickness. Micro-Raman spectroscopy was excited using a beam of 532 nm wavelength from an Ar laser in the 900 to 1900 cm^{-1} wavenumber range fitted by so-called D and G peaks using a Gaussian-curve function. The root mean square (RMS) roughness of the films was measured by contact-mode atomic force microscopy (AFM) over a fixed sampling area of 1×1 μm^2. The RMS roughness value for each sample was an average of five measurements at different positions, and the error was estimated to be about 0.1 nm. A ball-on-disk tribometer with a 1.27 cm (1/2 in) AISI 52100 chrome steel ball under a 1 N load was used to determine the unlubricated sliding friction coefficient. The maximum number of contact cycles was 25,000.

Results and Discussion

Fig. 1 shows the Raman spectra of the pure DLC and Si-DLC (7 at.% and 15 at.% Si) films deposited onto silicon substrates. In the Raman spectrum of amorphous carbon, the G band (~ 1580 cm^{-1}) and D band (~ 1350 cm^{-1}) were attributed to the E_{2g} stretching vibration and the disordering of ordered graphite structure, respectively [13]. It is clearly evident that the G peak position shifted towards a lower wavenumber when the Si content increased from 0 to 15 at.%. This confirms that Si incorporation can facilitate the formation of sp^3 bonded carbon sites in the amorphous DLC matrix [14].

Typical plots of the Raman spectra changes of the pure DLC, 7 at.% and 15 at.% Si-DLC films versus the different annealing temperatures are shown in Figs. 2(a)-4(a). Also included are cross-sectional SEM images of the films annealed at the various temperatures in ambient air (Figs. 2(b)-4(b)).

Fig. 2(a) shows the Raman spectra of the pure DLC films after thermal annealing. As is apparent, the spectrum did not change until 200 °C annealing. However, the D and G peak separation initiated at an annealing temperature of 300 °C and then was apparent at 400 °C, indicating a pronounced transformation of sp^3 bonded carbon to sp^2 bonded carbon [15-17]. Clearly, the film thickness of the pure DLC decreased with increasing annealing temperature (Fig. 2(b)). Then, after annealing at 400 °C it decreased to about 300 nm, and when annealed at 500 °C, the film disappeared. Yang et al. [10] reported a dependence of thickness variation on the composition of DLC and DLN films. They showed that oxygen from air was
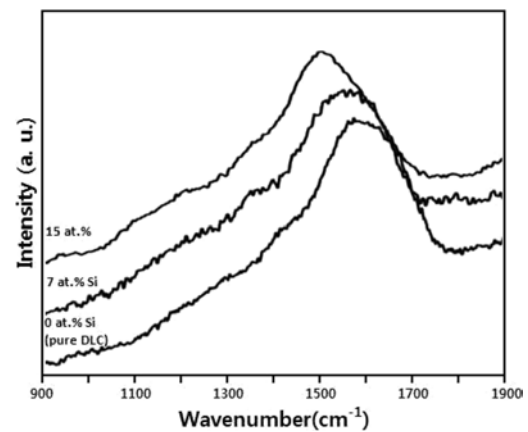
Fig. 1. Raman spectra of DLC films as function of Si content.
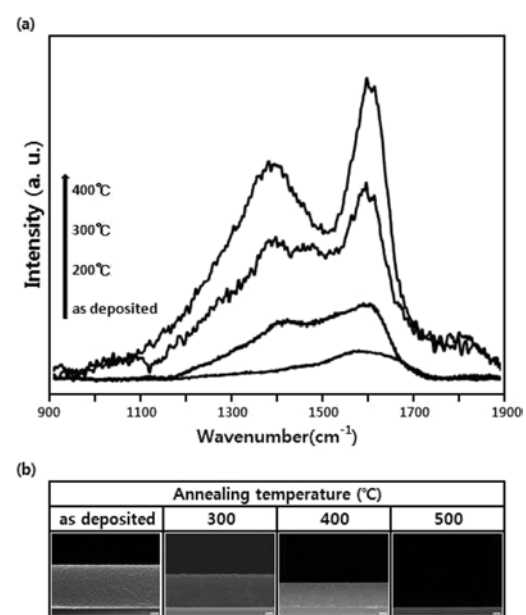
Fig. 2. (a) Raman spectra of pure DLC films annealed at various temperatures. (b) Corresponding cross-sectional FESEM images of pure DLC films. All of the scale bars are 100 nm.

adsorped into the film surface during the annealing process, forming carbon dioxide, after which it was completely effused out from the surface. This oxidation reaction results in decreased of film thickness during annealing in an air atmosphere. It is well known also that thermal degradation of DLC films initiates by means of a strong hydrogen loss upon high temperature annealing [2]. Therefore, pure DLC's loss of film thickness is likely due to effusion of carbon dioxide and hydrogen from the film surface.

Fig. 3(a) show the Raman spectra of the 7 at.% Si-DLC films after annealing at various temperatures. For these films, the D and G peak separation was not significantly changed until annealing at 300 °C, and became observable above 400 °C. The corresponding cross-sectional FESEM images shown in Fig. 3(b) reveal that the 7 at.% Si-DLC films persisted on the substrates to an 80 nm thickness until 700 °C annealing.
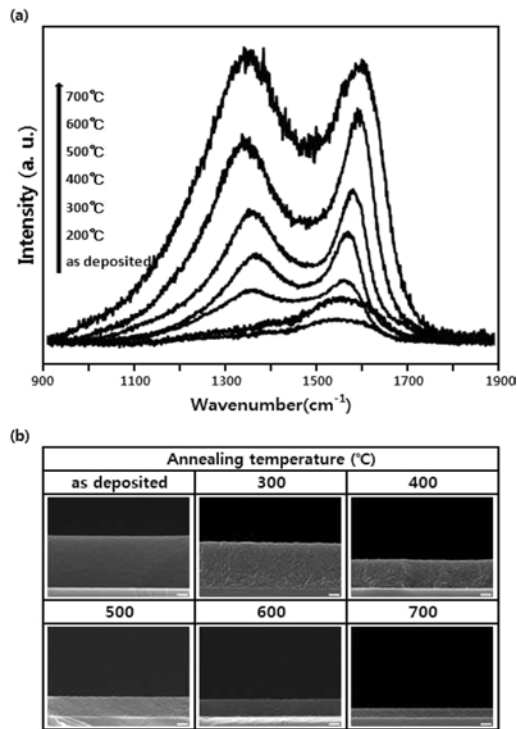
Fig. 3. (a) Raman spectra of 7 at.% Si-DLC films annealed at various temperatures. (b) Corresponding cross-sectional FESEM images of 7 at.% Si-DLC films. All of the scale bars are 100 nm.
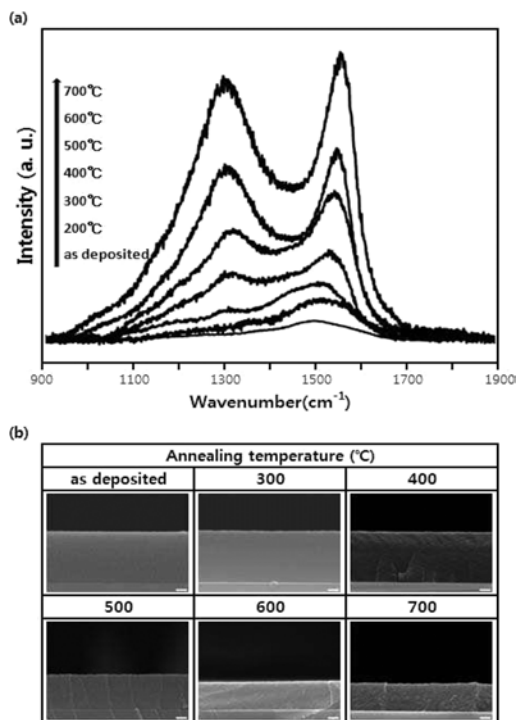
Fig. 4. (a) Raman spectra of 15 at.% Si-DLC films annealed at various temperatures. (b) Corresponding cross-sectional FESEM images of 15 at.% Si-DLC films. All of the scale bars are 100 nm.

Fig. 4(a) shows the Raman spectra of the 15 at.% Si-DLC films annealed at different temperatures. As is evident, the annealing temperature effecting significant
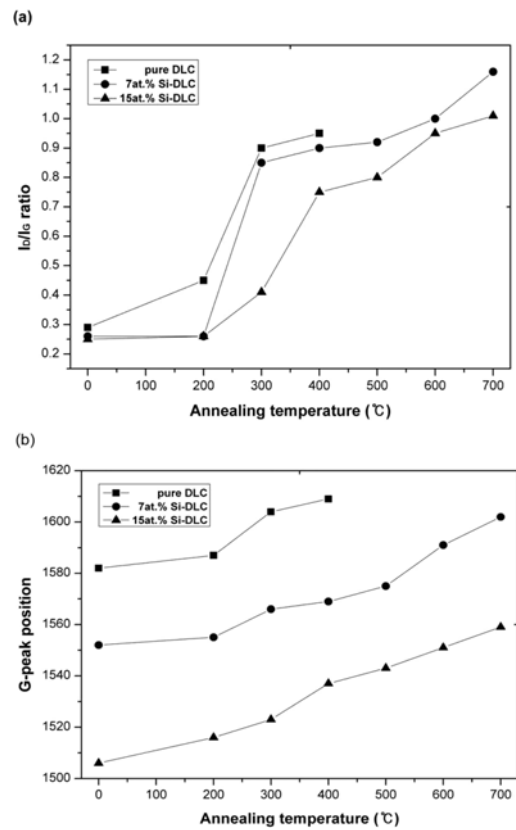
Fig. 5. Variation of I_D/I_G ratio and G peak position as calculated from Raman spectra of pure DLC and Si-DLC films as function of annealing temperature: (a) I_D/I_G ratio, (b) G peak position.

splitting of the D and G peaks was higher than that for the 7 at.% Si-DLC films. Furthermore, as shown in Fig. 4(b), the 15 at.% Si-DLC films maintained a thickness of 300 nm after 700 °C annealing. As indicated by the Raman spectra of the Si-DLC films (Figs. 3(a) and 4(a)), Si incorporation formed more sp^3 bonded carbon and stabilized the structure, enabling graphitization at higher temperatures than in the case of pure DLC films.

As mentioned above, with the pure DLC films, the reaction between carbon and oxygen at high annealing temperatures resulted in thickness loss and finally, disappearance (Fig. 2(b)). The Si incorporated films, by contrast, showed no appreciable thickness loss up to 500 °C, in fact, at 700 °C, the films, most notably the 15 at.% Si, still maintained 60% of their thickness. It is recognized that the effects of Si incorporation into DLC films are generally attributable to Si-C bond formation [14]. In our previous study [12], we observed the formation of Si-C nanocrystallites (β-SiC) upon Si incorporation into DLC films, which were stable even after high temperature RTP annealing. If a reaction between Si-C and oxygen occurs by oxidation, silicon dioxide (the Si-O network) will be formed as a by-product. The silicon dioxide remains on the Si-DLC films, acting as a barrier layer preventing diffusion of oxygen [7, 10]. Recently, Nakazawa et al. employed XPS and FTIR to confirm formation of the Si-C bond
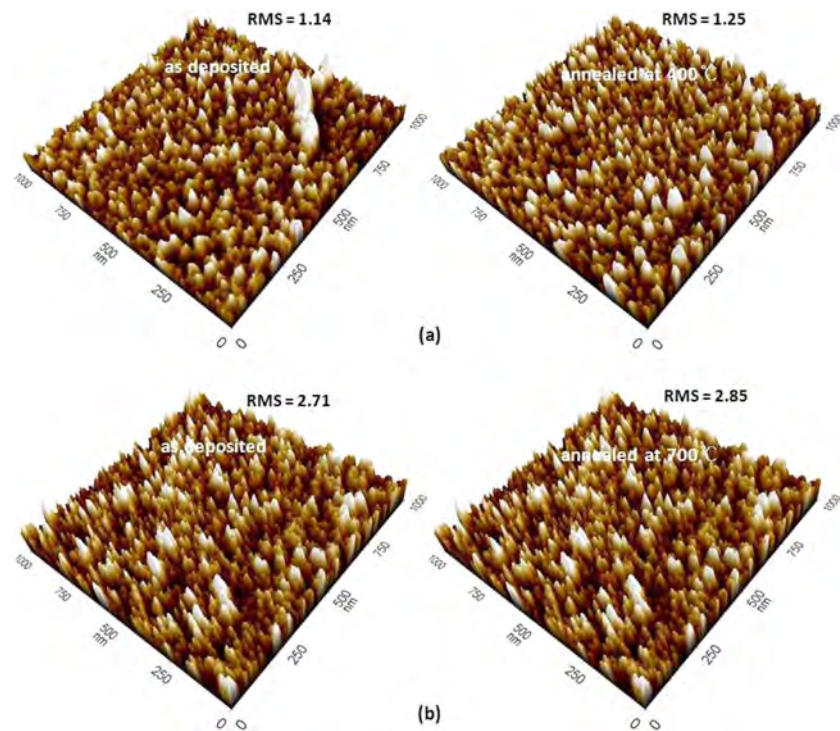
Fig. 6. (a) AFM images of pure DLC films before annealing and after 400 °C annealing. (b) AFM images of 15 at.% Si-DLC films before annealing and after 700 °C annealing.

in pulsed-laser-deposited Si-DLC films [18]. Thus, it expected that silicon dioxide formed on 15 at.% Si-DLC films during the annealing process prevents film reduction even at temperature as high as 700 °C (Fig. 4(b)).

The Raman spectra were analyzed by the Gaussian curve fitting method to evaluate the structural changes of the pure DLC and Si-DLC films with annealing temperature. Fig. 5 (a) and (b) show the variation of the corresponding I_D/I_G ratios and the G peak positions for the annealed pure DLC and Si-DLC films, respectively. It is apparent that in all of the cases, as the annealing temperature increased, the I_D/I_G ratio increased and the G peak shifted towards a higher wavenumber, indicating that the annealed films contained relatively higher sp^2 contents than the as-deposited films. Such an increase of I_D/I_G ratio and G peak shift as a result of the observable separation of the D and G peaks (Fig. 2(a)-4(a)) results in a considerable transformation of the sp^3 bonds to sp^2 bonds, indicating an increase of the random network of nanocrystalline graphite as the annealing temperature increases. Similar behavior has been observed in previous studies on the thermal stability of Si-DLC films [3, 12, 19]. However, the graphitization (sp^3-to-sp^2 transition) temperature of Si-DLC films, which increases as the Si content increases, is higher than that of pure-DLC films. From Raman analysis and a study of thickness change as a function of annealing temperature, it can be deduced that Si-DLC films show, in comparison with pure DLC films, good thermal stability of their applied protective
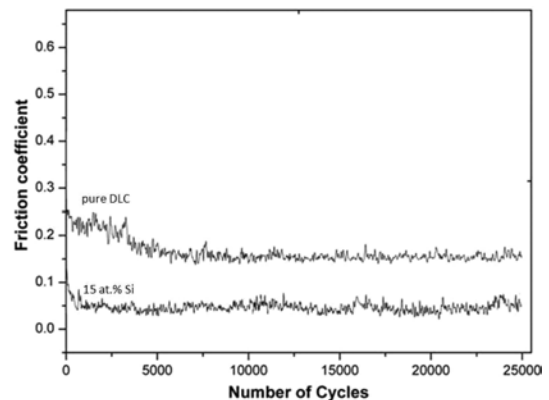
Fig. 7. Evolution of friction coefficient of pure DLC and 15 at.% Si-DLC films against steel ball in ambient air.

coating at high temperatures in ambient air.

Fig. 6(a) shows three-dimensional AFM images of the pure DLC films before annealing and after 400 °C annealing. Fig. 6(b) shows corresponding images of the 15 at.% Si-DLC films before annealing and after 700 °C annealing. As indicated in Figs. 2(a) and 4(a), the annealed samples showed nearly the same thickness, about 300 nm. In all of the cases, the film roughness ranged from 1.14 nm to 2.85 nm, as reflected the fact that the Si-DLC films had maintained their smooth surface after annealing.

Fig. 7 plots the friction coefficient of the as-deposited pure DLC and 15 at.% Si-DLC films in ambient air at room temperature. All of the films showed nearly constant values of friction coefficient until a final

sliding of the ball on the film surface. The friction coefficient of the pure DLC films was 0.17, whereas that of the 15 at.% Si-DLC films was a low value of 0.05, indicating good friction properties. It is well known that the most frequently observed low friction coefficient mechanism between Si-DLC films and a steel ball, in various environments, might be due to the formation of a SiO_2 lubricant layer, that possibly arises from friction-produced oxidation [20, 21]. It would be prudent then to investigate, for reliable long-term performance, Si-DLC films' thermal stability with respect to structural change at elevated temperatures along with their low friction mechanism.

Conclusions

The more Si is incorporated into films, the higher is graphitization temperature than for pure DLC films. This hypothesis was confirmed in the present study's results, which included increases of the D and G peak separation temperature, the I_D/I_G ratio, and the G peak position. In the case of the pure DLC films, the reaction between carbon and oxygen at high annealing temperatures resulted in a considerable loss of thickness, whereas the 15 at.% Si-DLC films showed no remarkable loss up to 500 °C, indeed, the smooth-surface films maintained 60% of their thickness even after 700 °C annealing. The formation of silicon dioxide by oxidation of SiC nanocrystallites on the Si-DLC films effects a significant thermal stability improvement of such films.

References

1. J.C. Damasceno, S.S. Camargo Jr., F.L. Freire Jr. and R. Carius, Surf. Coat. Technol. 133-134 (2000) 247-252.
2. S.S. Camargo Jr., R.A. Santos, A.L.B. Neto, R. Carius and F. Finger, Thin Solid Films 332 (1998) 130-135.
3. W.J. Wu and M.H. Hon, Surf. Coat. Technol. 111 (1999) 134-140.
4. C.S. Lee, K.R. Lee, K.Y. Eun, K.H. Yoon and J.H. Han, Diamond Relat. Mater. 11 (2002) 198-203.
5. R.D. Evans, G.L. Doll, P.W. Morrison Jr., J. Bentley, K.L. More and J.T. Glass, Surf. Coat. Technol. 157 (2002) 197-206.
6. V. Kulikovsky, P. Bohac, J. Zemek, V. Vorlieek, A. Kurdyumov and L. Jastrabik, Diamond Relat. Mater. 16 (2007) 167-173.
7. S. Zhang, X.L. Bui and X. Li, Diamond Relat. Mater. 15 (2006) 972-976.
8. A. Bendavid, P.J. Martin, C. Comte, E.W. Preston, A.J. Haq, F.S. Magdon Ismail and R.K. Singh, Diamond Relat. Mater. 16 (2007) 1616-1622.
9. Ricky K.Y. Fu, Y.F. Mei, M.Y. Fu, X.Y. Liu and Paul K. Chu, Diamond Relat. Mater. 14 (2005) 1489-1493.
10. W.J. Yang, Y.H. Choa, T. Sekino, K.B. Shim, K. Niihara and K.H. Auh, Thin Solid Films 434 (2003) 49-54.
11. A. Varma, V. Palshin and E.I. Meletis, Surf. Coat. Technol. 148 (2001) 305-314.
12. K.H. Er and M.G. So, J. Ceram. Proc. Res. 11 (2010) 760-764.
13. A. Richter, H.J. Scheibe, W. Pompe, K.W. Brzezinka and I. Muhling, J. Non-Cryst. Solids 88 (1986) 131-144.
14. J.F. Zhao, P. Lemoine, Z.H. Liu, J.P. Quinn and J.A. McLaughlin, J. Phys.: Condens. Matter 12 (2000) 9201-9213.
15. A.C. Ferrari and J. Robertson, Phys. Rev. B 61 (2000) 14095-14107.
16. C. Casiraghi, A.C. Ferrari and J. Robertson, Phys. Rev. B 72 (2005) 0854011-08540113.
17. G. Irmer and A.D. Reisel, Adv. Eng. Mater. 7 (2005) 694-705.
18. H. Nakazawa, R. Osozawa, T. Okuzaki, N. Sato, M. Suemitsu and T. Abe, Diamond Relat. Mater. 20 (2011) 485-491.
19. H.W. Choi, D.M. Gage, R.H. Dauskardt, K.R. Lee and K.H. Oh, Diamond Relat. Mater. 18 (2009) 615-619.
20. S.S. Camargo Jr., J.R. Gomes, J.M. Carrapichano, R.F. Silva and C.A. Achete, Thin Solid Films 482 (2005) 221- 225.
21. J. Choi, S. Nakao, S. Miyagawa, M. Ikeyama and Y. Miyagawa, Surf. Coat. Technol. 201 (2007) 8357-8361.